Free Radical Research, September 2009; 43(9): 796–802

informa
healthcare

Direct, real-time monitoring of superoxide generation in isolated mitochondria

JAMES R. HENDERSON[1], HELEN SWALWELL[2], SARAHJAYNE BOULTON[1], PHILIP MANNING[1], CALUM J. MCNEIL[1], & MARK A. BIRCH-MACHIN[2]

[1]*Diagnostic & Therapeutic Technologies, and* [2]*Dermatological Sciences, Institute of Cellular Medicine, Newcastle University, NE2 4HH, UK*

(Received 18 March 2009; in revised form 21 May 2009)

Abstract
Mitochondria are one of the major sources of reactive oxygen species (ROS) in mammalian cells. The generation of ROS underlies many physiological and pathophysiological processes that occur within cellular systems. Superoxide (O_2^-) is the proximal ROS generated during electron 'leakage' from the mitochondrial electron transport chain (mETC) and is known to be released at mitochondrial complex I and complex III. Monitoring mitochondrial O_2^- production directly and in real-time offers the potential to improve understanding of the complex mechanisms involved during mitochondrial O_2^- generation. This study reports the novel application of a cytochrome *c* functionalized amperometric sensor for monitoring O_2^- generation in isolated mitochondrial fractions. The non-invasive sensor system described allowed a comparison of O_2^- production following specific inhibition of complex I and complex III of the mETC to be made directly and in real-time.

Keywords: *Superoxide, isolated mitochondria, amperometric detection, complex I, complex III*

Abbreviations: *ROS, reactive oxygen species; mETC, mitochondrial electron transport chain; SOD, superoxide dismutase; XOD, xanthine oxidase; DTSSP, 3,3′-dithiobis(sulphosuccinimidylpropionate); EPR, electron paramagnetic resonance*

Introduction

The primary function of mitochondria is to carry out oxidative phosphorylation. Complexes I–IV of the mitochondrial electron transport chain (mETC) transfer electrons from reduced substrates to oxygen, coupled to the creation of a proton gradient across the inner mitochondrial membrane [1–3]. It is well established that the mETC is the major cellular generator of superoxide (O_2^-) as a result of leakage of single electrons which reduce O_2 to form O_2^- [4].

Superoxide is the proximal reactive oxygen species (ROS) generated in mitochondria [5] and it can be readily converted into other ROS, as summarized in Figure 1. Reactive oxygen species are involved in a number of cellular processes under normal physiological conditions, such as cell signalling [6]. However, when cellular production of ROS is greater than the antioxidant capacity, O_2^- and other ROS become a major cause of cellular oxidative damage. This 'oxidative stress' causes damage to macromolecules such as lipids, proteins and DNA [7] and it is a mechanism that has significance in many degenerative diseases as well as ageing [8]. ROS within cells are known to act as secondary messengers in intracellular signalling cascades, which induce and maintain the oncogenic phenotype of cancer cells. Redox imbalances have been found to be present in many cancer cells compared with normal cells [9]. Thus, redox imbalance may be related to oncogenic stimulation.

There is evidence that most of the O_2^- generated by the mETC originates from complexes I and III [10],

Correspondence: Professor Calum McNeil, Diagnostic & Therapeutic Technologies, Institute of Cellular Medicine, Newcastle University, Newcastle upon Tyne NE2 4HH, UK. Fax: +44(0)191 222 7991. Email: calum.mcneil@newcastle.ac.uk

ISSN 1071-5762 print/ISSN 1029-2470 online
DOI: 10.1080/10715760903062895

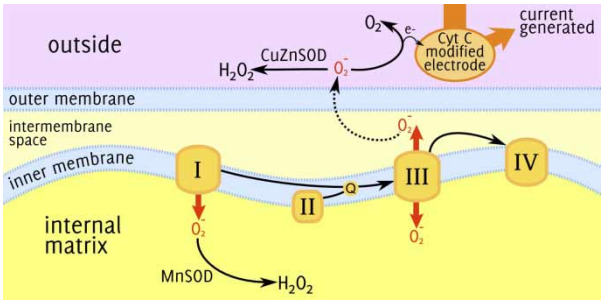

Figure 1. Generation of O_2^- and other reactive oxygen species in the mitochondrial electron transport chain.

although the relative contribution of these complexes to O_2^- production and the possible involvement of other complexes remains to be fully elucidated [4].

Since O_2^- is involved in many cellular processes, both physiological and pathophysiological, direct, real-time monitoring of its production offers greater insight into the temporal and spatial aspects of O_2^- generation in biological systems. A number of methods have been employed to monitor O_2^- production *in vitro* including fluorescence [11,12] and electrochemical [13–15] techniques. Mitochondria are the predominant source of O_2^- generated in mammalian cells and, as such, monitoring the organelles directly offers the potential to enhance our understanding of cellular damage following increased O_2^- production. The application of both fluorescence and electroparamagnetic resonance (EPR) methods have been used to monitor O_2^- production in isolated mitochondria [16–19]. However, as yet, amperometric sensors have not been used for the direct, real-time monitoring of O_2^- generation in isolated mitochondrial fractions. The covalent attachment of the redox protein cytochrome *c* to the surface of gold electrodes has been reported extensively for qualitatively monitoring O_2^- dynamics *in vitro* [11,13–15,20–24]. Such an approach offers a number of significant advantages over spectrophotometric or chemiluminescent methods. The principle advantage of this technique is the ability to measure O_2^- production from whole cells or isolated organelles directly and in real-time. This overcomes the limitations of more traditional 'end-point' analysis which relies on the measurements of reaction products or adducts. In addition the high degree of selectivity that the amperometric electrode shows for O_2^- in the presence of non-specific reducing agents such as ascorbic acid has been extensively reported [11,13–15,20–24]. This selectivity has been primarily attributed to a low operating potential of +100 mV (vs Ag/AgCl reference electrode) [11,13–15,20–24]. Additionally, measurements made with the electrode do not involve the addition of dyes or substrates to the cellular environment which could adversely influence cellular observations.

Reported here is the novel use of chronoamperometry to specifically detect, directly and in real-time O_2^- production from the mitochondrial electron transport chain. A greater understanding of the role of mitochondrial O_2^- production may ultimately lead to a fuller understanding of many important disease pathways and the identification of novel targets for drug therapy. The data presented here clearly demonstrates the potential of a cytochrome *c* functionalized sensor to delineate these pathways.

Materials and methods

Reagents

Antimycin A, cytochrome *c*, rotenone, superoxide dismutase (SOD), xanthine and xanthine oxidase (XOD) were purchased from Sigma-Aldrich (Poole, UK). 3,3′-Dithiobis(sulphosuccinimidylpropionate) (DTSSP) was supplied by Pierce (Chester, UK).

Cell culture

The melanoma cell line FM55 (a kind gift from Professor Des Tobin, Bradford University, UK) was cultured in Dulbecco's modified Eagle's medium (Lonza, UK) supplemented with 10% foetal calf serum, 100 U/mL streptomycin (Invitrogen, UK), and 0.1 mg/mL penicillin (Invitrogen, UK), in a humidified atmosphere with 5% (v/v) CO_2 at 37°C. The medium was changed every 2–3 days. Cells were grown to near confluence in 150 cm^2 flasks to six passages prior to isolation of mitochondria.

Mitochondrial fraction preparation

An enriched mitochondrial fraction was isolated from cultured cells by physical homogenization, differential centrifugation and treatment with hypotonic buffer. Cultured cells were harvested and washed with phosphate buffered saline (PBS). All subsequent procedures were carried out on ice or at 4°C. The washed pellet was resuspended in 1 mL of a sucrose rich mitoprep buffer (pH7.4) containing 250 mM sucrose (Sigma-Aldrich, UK), 2 mM HEPES (Sigma-Aldrich, UK) and 0.1 mM EGTA (Sigma-Aldrich, UK) and disrupted by 20 passes in a power-driven Teflon-glass homogenizer. The homogenate was centrifuged for 10 min at 2200 rpm at 4°C and the supernatant collected. The supernatant was then centrifuged at 11 000 rpm for 10 min at 4°C. The resulting pellet containing the mitochondrial fraction was resuspended in mitoprep buffer and stored in aliquots at −80°C until use [25]. Protein concentration was determined using the Bradford assay (Bio-Rad, UK) as per the manufacturer's instructions. The isolated mitochondria were maintained in the sucrose rich buffer during all electrochemical measurements.

Superoxide responsive electrode preparation

The cytochrome *c* based O_2^- electrode was prepared as previously described [15]. In brief, a 2 mm O.D. solid gold electrode (BioAnalytical Systems, Cambridgeshire, UK) was polished using 0.02 μm aluminium oxide slurry on a 'micro-cloth' cleaning platform (BioAnalytical Systems, Cambridgeshire, UK) and sonicated for 5 min. The electrode was then incubated in a 50 mM solution of DTSSP for 5 min at room temperature before being gently rinsed in distilled water. Finally, the electrode was incubated in a 2 mM cytochrome *c* solution (in PBS, pH 7.4) at 4°C overnight. The modified electrode was rinsed immediately before use and calibrated using the reaction between xanthine and XOD to generate O_2^- as described previously [14,15]. For all amperometric measurements the electrode was coupled with a Ag/AgCl electrode that acted as both reference and counter electrode (Harvard Apparatus, Edenbridge, UK). The electrodes were connected to an in-house potentiostat interfaced with a PC coupled with data acquisition software. All measurements were carried out at +100 mV operating potential (vs Ag/AgCl electrode). For calibration the functionalized electrode was placed in 990 μL of 10 mM xanthine solution (in 100 mM KOH) and a steady baseline current was observed. To this 10 μL of varying concentrations of XOD (0.5, 1, 2, 3, 4 or 5 μM) were added and any change in current was recorded.

Monitoring superoxide generation from isolated mitochondria

The same electrode set-up was used for monitoring O_2^- generation from isolated mitochondria as that described for calibrating the electrode. A 100 μL suspension of isolated mitochondria (0.162 μg/mL protein concentration) was placed into a sterile conical well and the electrode lowered directly into the suspension, completely immersing the functionalized surface of the electrode. A steady baseline current was observed before adding 15 μL of either 100 μM antimycin A or 100 μM rotenone to inhibit mitochondrial complex III or complex I, respectively. Any subsequent current change was recorded. To demonstrate specificity of the electrode for O_2^-, the electrode was placed into 100 μL of isolated mitochondria (0.487 μg/mL protein concentration) and 15 μL of antimycin was added. Approximately 30 s after the addition of antimycin A was made, 15 μL of 7500 U/mL SOD was added to scavenge any O_2^- generated by the sample. As a further demonstration of specificity, the electrode was lowered into a 100 μL suspension of isolated mitochondria that contained 7500 U/mL SOD. As before, a steady baseline current response was observed before 15 μL of 100 μM antimycin A was added.

Results

Superoxide electrode calibration

The electrode response was examined using the enzymatic reaction between XOD with its substrate, xanthine, under conditions of substrate saturation to generate O_2^-. The change in current observed was calculated as current density (nA μM^{-1} cm^{-2}). The electrode response was shown to be linearly dependent upon XOD concentration (Figure 2) and therefore proportional to the amount of O_2^- generated. Calibration data presented in Figure 2 are in keeping with those reported previously [14,15].

Monitoring superoxide generation from isolated mitochondria

The production of O_2^- by isolated mitochondria was monitored successfully using the cytochrome *c* functionalized electrode. Any change in current observed was directly proportional to the amount of O_2^- present. Figure 3 represents two typical responses following inhibition of mitochondrial complexes I and III. The inhibition of complex III through the addition of antimycin A brought about an immediate increase in O_2^- generation leading to a rapid increase in current which peaked at 30.53 nA above the pre-addition baseline (Figure 3A). The current response stabilized within 120 s and a continuous current of ~4 nA was observed for the remainder of each experiment. In contrast, inhibition of complex I through the addition of rotenone induced a comparatively small increase in current, reaching a maximum of 10.99 nA above the pre-addition baseline, indicating much lower peak O_2^- generation (Figure 3B). Additionally the response returned to pre-stimulus baseline levels within 90 s.

To demonstrate the specificity of the electrode for O_2^-, isolated mitochondria were stimulated with antimycin A, as this consistently elicited the largest

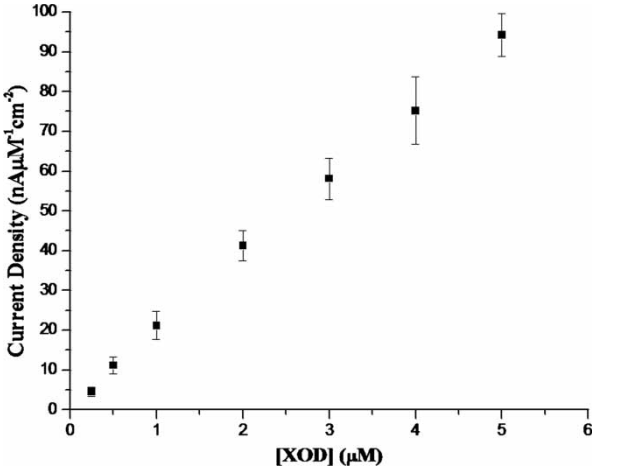

Figure 2. Calibration of a cytochrome *c* functionalized electrode through the enzymatic generation of O_2^- ($n = 3 \pm SD$).

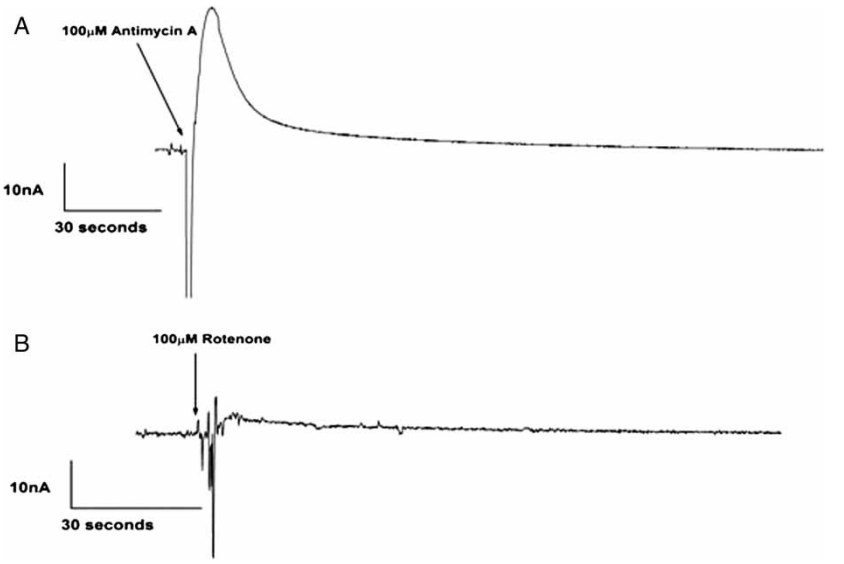

Figure 3. The time course of antimycin A (A) and rotenone (B) induced O_2^- generation in isolated mitochondrial fractions. The increase in current observed was proportional to the flux of O_2^- generated during mitochondrial inhibition.

O_2^- response. As in Figure 3A, the addition of antimycin A to the isolated mitochondria sample induced a rapid increase in O_2^- generation leading to a current peak 44.70 nA above the pre-addition baseline. Approximately 30 s after the addition of antimycin A, 7500 U/mL SOD was added to the sample. The presence of the O_2^- scavenger brought about an immediate decrease in current as the O_2^- generated through the inhibition of complex III was scavenged (Figure 4A). The current response re-stabilized below the original baseline value. The addition of antimycin A to mitochondrial samples already containing SOD did not induce an increase in O_2^- generation detectable by the electrode (Figure 4B). A slight change in current was observed as the antimycin A was added to the sample, but the current returned to the baseline level within 5 s.

Discussion

In this study the application of a cytochrome *c* functionalized gold electrode to monitor O_2^- production in isolated mitochondria has been reported. This method allowed the dynamics of mitochondrial O_2^- release following the specific inhibition of complex I and complex III of the mETC to be examined comparatively and in real-time.

Antimycin A is known to inhibit complex III by binding to the complex at centre '*I*' and blocking the electron transfer from centre '*o*' of the Q cycle, forming semi-quinone that reduces oxygen to O_2^- [8,18,26]. The large and immediate increase in O_2^- production observed during the inhibition of complex III with antimycin A (Figure 3A) is in keeping with this previously reported work [8,18,26]. Complex III is known to asymmetrically generate O_2^- that passes both into the matrix and into the inter-membrane space of the mitochondrion. However O_2^-, once in its anionic form, is too strongly charged to readily cross the mitochondrial inner membrane [26–29]. Thus, superoxide production exhibits a distinct membrane sidedness or 'topology'. In addition, the electron acceptor associated with complex III is cytochrome *c*, which is located on the outer part of the inner membrane and, therefore, explains the superoxide production into the inter-membrane space (Figure 1). Furthermore, it has been known for some time that partial turnover of the cyt bc_1 components within complex III in the presence of antimycin A, a Q(i) site inhibitor, results in accumulation of a semiquinone at the Q(o) site, which can result in superoxide production on the outer aspect of the inner membrane adjacent to the inter-membrane space [30,31]. As a result of these combined features the O_2^- detected by the electrode will be that released outside the inner membrane (Figure 1). This sidedness or topology of O_2^- production is the basis for the measurement of O_2^- production at complex III using the end point EPR spin trap, 5,5-dimethyl-1-pyrroline *N*-oxide (DMPO), which, like the gold electrode employed in these studies, is external to the mitochondria and which detects increased O_2^- production effluxed outward following addition of antimycin A [32].

Superoxide generation at complex I can be attributed to electron leakage at the quinone binding site [33] and in the presence of a Q-site inhibitor (such as rotenone) the rate of O_2^- production can increase 10–30-fold [33]. In detail, rotenone is believed to block electron transfer from the N2 iron-sulphur cluster to ubiquinone [34]. However, as O_2^- generated at complex I is released exclusively into the mitochondrial matrix [27,33,35], O_2^- should

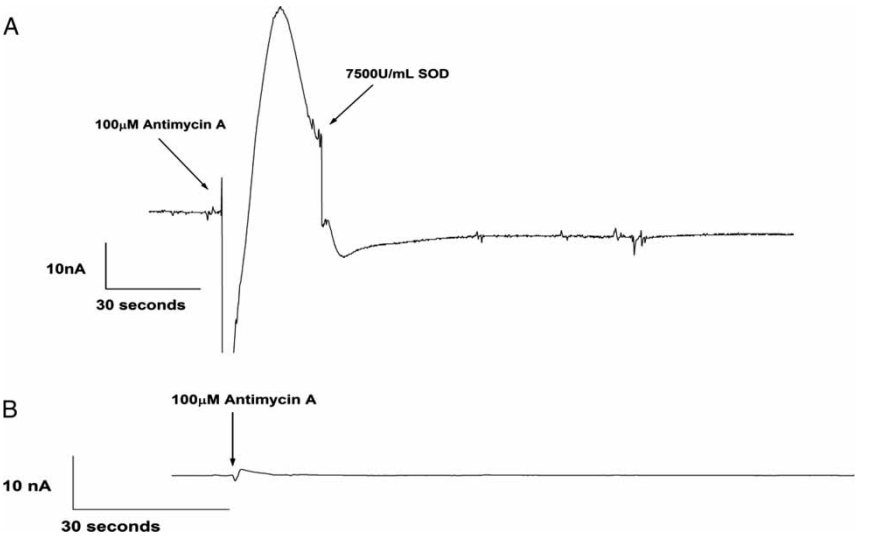

Figure 4. Scavenging of O_2^- following the addition of 7500 U/mL SOD to antimycin A activated isolated mitochondria. The rapid drop in current following SOD addition demonstrates the specificity of the electrode for O_2^- (A). No increase in O_2^- generation was observed in response to antimycin A in isolated mitochondria samples that already contained SOD (B).

not be detected by the electrochemical method. Consistent with this, inhibition of complex I by rotenone (Figure 3B) produced a much smaller change in current than that observed during complex III inhibition (Figure 3A). However, the low permeability of the mitochondrial membrane to O_2^- would suggest that no O_2^- would be detected by the electrode following the addition of rotenone, yet the change in current observed demonstrates that some O_2^- was produced (Figure 3B). The O_2^- detected following the addition of rotenone may have been generated from upstream sites in complex I, as the site of action for rotenone is thought to be in the distal position of the complex [32]. In this respect there is good evidence from inhibitor analysis studies [36] showing efficient redox cycling at two sites within complex I, one proximal and one distal to the putative rotenone binding site. Alternatively, the O_2^- produced could be derived from semi-quinone formation at complex III, as reported by O'Malley et al. [32]. Further investigation into the mechanisms of complex I associated O_2^- production may clarify the findings reported in these studies.

The *in vitro* specificity of the electrode for O_2^- has been reported previously [11,15,20] and this was confirmed in this study through the addition of SOD before and after induction of O_2^- generation (Figure 4A and B). The re-stabilization of the current response at a level below the pre-inhibition baseline observed in Figure 4A can be accounted for by the presence of O_2^- in the sample prior to antimycin A addition. Electrons would have been 'leaking' from the mETC at low levels, therefore generating small amounts of O_2^- in the mitochondrial sample as the electrode was polarizing to a steady baseline current response. As SOD has such a high affinity for O_2^-, scavenging of the radical would have been comprehensive leading to a drop in current response below the initial baseline value as most of the O_2^- present in the sample was completely scavenged. The specificity of the electrode was further confirmed by the presence of SOD prior to induction of O_2^- generation (Figure 4B). By including SOD in the sample before inhibiting the mETC, any O_2^- generated would be scavenged before reaching the cytochrome *c* immobilized at the electrode surface, hence no change in current was recorded. Importantly, the addition of SOD also demonstrated that the electrode was not responsive to H_2O_2, which is spontaneously generated during dismutation of O_2^-.

It is worth noting that the current response observed following the addition of both rotenone and antimycin A to isolated mitochondria was much larger than would be expected in whole cell samples [13,15,20]. This is not surprising considering that the antioxidant mechanisms that exist in cellular systems are not present in the mitochondrial fractions — O_2^- is rapidly converted to H_2O_2 by MnSOD in the mitochondrial matrix [37] or by Cu/ZnSOD in the intermembrane space and cytosol [38]. All cytosolic SOD was removed when the mitochondria were isolated from their normal cellular environment and there is evidence to suggest that any residual Cu/ZnSOD becomes inactive in isolated mitochondria [39,40]. It is therefore important to stress that all O_2^- production observed in this study was representative of the mitochondria as the O_2^- released should not be converted to H_2O_2 nor can it have been associated with other cellular O_2^- generating processes such as NAD(P)H oxidase, cytochrome P-450 or xanthine oxidase [35,41,42].

In conclusion, the application of amperometric O_2^- detection has been successfully applied to isolated mitochondrial fractions. A comparison of

O_2^- generation following specific inhibition of mitochondrial complex I and complex III was performed and the observations were in keeping with previous studies [18,26,29,34,43]. A possible future application of this detection method would be to examine O_2^- profiles of disease state cells vs wild type cells both *in vitro* and through the use of isolated mitochondrial fractions. However, it must be stressed that the capacity of cells or tissues to generate O_2^- will vary and this is influenced by factors such as age and localized concentrations of O_2^- producing enzymes. In addition, future studies must also consider the degree of control strength which the activity of the individual enzyme complex (i.e. complex I vs complex III) exerts on the whole pathway of electron transfer along the respiratory chain in the mitochondria. Using inhibitor analysis studies, we have previously shown that complex III exerts a different degree of control even between different cell types (muscle vs liver) [43]. It is, therefore, very difficult to extrapolate O_2^- generation data acquired from isolated mitochondrial fractions into *in vitro* O_2^- production. However, the data presented in this study has clearly demonstrated the analytical capabilities of amperometric sensing for the direct, real-time analysis of qualitative O_2^- generation from isolated mitochondria following the chemical modulation of electron transport complexes. This sensing technology has clear potential to greatly improve the current understanding of O_2^- flux *in vitro*.

Acknowledgements

The authors would like to thank the EPSRC/Royal Society of Chemistry Analytical Sciences scheme and Cancer Research UK (C1474/A10235) for providing funding for this study.

***Declaration of interest*:** The authors report no conflicts of interest. The authors alone are responsible for the content and writing of the paper.

References

[1] Chance B, Mela L. Proton movements in mitochondrial membranes. Nature 1966;212:372–376.
[2] Chance B, Mela L. A hydrogen ion concentration gradient in a mitochondrial membrane. Nature 1966;212:369–372.
[3] Chance B, Mela L. Hydrogen ion concentration changes in mitochondrial membranes. J Biol Chem 1966;241:4588–4599.
[4] Murphy MP. How mitochondria produce reactive oxygen species. Biochem J 2009;417:1–13.
[5] Beckman KB, Ames BN. The free radical theory of aging matures. Physiol Rev 1998;78:547–581.
[6] Thannickal VJ, Fanburg BL. Reactive oxygen species in cell signaling. Am J Physiol Lung Cell Mol Physiol 2000;279:L1005–L1028.
[7] Orrenius S, Gogvadze V, Zhivotovsky B. Mitochondrial oxidative stress: implications for cell death. Annu Rev Pharmacol Toxicol 2007;47:143–183.
[8] Brand MD, Affourtit C, Esteves TC, Green K, Lambert AJ, Miwa S, Pakay JL, Parker N. Mitochondrial superoxide: production, biological effects, and activation of uncoupling proteins. Free Radic Biol Med 2004;37:755–767.
[9] Valko M, Rhodes CJ, Moncol J, Izakovic M, Mazur M. Free radicals, metals and antioxidants in oxidative stress-induced cancer. Chem-Biol Interact 2006;160:1–40.
[10] Raha S, Robinson BH. Mitochondria, oxygen free radicals, disease and ageing. Trends Biochem Sci 2000;25:502–508.
[11] Chang SC, Rodrigues NP, Zurgil N, Henderson JR, Bedioui F, McNeil CJ, Deutsch M. Simultaneous intra- and extracellular superoxide monitoring using an integrated optical and electrochemical sensor system. Biochem Biophys Res Commun 2005;327:979–984.
[12] Henderson LM, Chappell JB. Dihydrorhodamine 123: a fluorescent probe for superoxide generation? Eur J Biochem 1993;217:973–980.
[13] Aitken GR, Henderson JR, Chang SC, McNeil CJ, Birch-Machin MA. Direct monitoring of UV-induced free radical generation in HaCaT keratinocytes. Clin Exp Dermatol 2007;32:722–727.
[14] Cooper JM, Greenough KR, McNeil CJ. Direct electron transfer reactions of immobilized cytochrome c at modified gold electrodes. J Electroanal Chem 1993;347:267–275.
[15] Manning P, McNeil CJ, Cooper JM, Hillhouse EW. Direct, real-time sensing of free radical production by activated human glioblastoma cells. Free Radic Biol Med 1998;24:1304–1309.
[16] Elks CM, Mariappan N, Haque M, Guggilam A, Majid DS, Francis J. Chronic NF-κB blockade reduces cytosolic and mitochondrial oxidative stress and attenuates renal injury and hypertension in SHR. Am J Physiol 2009;296:F298–F305.
[17] Mariappan N, Elks CM, Fink B, Francis J. TNF-induced mitochondrial damage: a link between mitochondrial complex I activity and left ventricular dysfunction. Free Radic Biol Med 2009;46:462–470.
[18] Xu X, Arriaga EA. Qualitative determination of superoxide release at both sides of the mitochondrial inner membrane by capillary electrophoretic analysis of the oxidation products of triphenylphosphonium hydroethidine. Free Radic Biol Med 2009;46:905–913.
[19] Du G, Mouithys-Mickalad A, Sluse FE. Generation of superoxide anion by mitochondria and impairment of their functions during anoxia and reoxygenation *in vitro*. Free Radic Biol Med 1998;25:1066–1074.
[20] Chang SC, Pereira-Rodrigues N, Henderson JR, Cole A, Bedioui F, McNeil CJ. An electrochemical sensor array system for the direct, simultaneous in vitro monitoring of nitric oxide and superoxide production by cultured cells. Biosens Bioelectron 2005;21:917–922.
[21] Datta HK, Manning P, Rathod H, McNeil CJ. Effect of calcitonin, elevated calcium and extracellular matrices on superoxide anion production by rat osteoclasts. Exp Physiol 1995;80:713–719.
[22] Manning P, Cookson MR, McNeil CJ, Figlewicz D, Shaw PJ. Superoxide-induced nitric oxide release from cultured glial cells. Brain Res 2001;911:203–210.
[23] McNeil CJ, Manning P. Sensor-based measurements of the role and interactions of free radicals in cellular systems. Rev Mol Biotech 2002;82:443–455.
[24] McNeil CJ, Smith KA, Bellavite P, Bannister JV. Application of the electrochemistry of cytochrome c to the measurement of superoxide radical production. Free Radic Res Commun 1989;7:89–96.

[25] Kirby DM, Thorburn DR, Turnbull DM, Taylor RW. Biochemical assays of respiratory chain complex activity. Methods Cell Biol 2007;80:93–119.
[26] Muller FL, Liu Y, Van Remmen H. Complex III releases superoxide to both sides of the inner mitochondrial membrane. J Biol Chem 2004;279:49064–49073.
[27] St-Pierre J, Buckingham JA, Roebuck SJ, Brand MD. Topology of superoxide production from different sites in the mitochondrial electron transport chain. J Biol Chem 2002;277:44784–44790.
[28] Miwa S, St-Pierre J, Partridge L, Brand MD. Superoxide and hydrogen peroxide production by Drosophila mitochondria. Free Radic Biol Med 2003;35:938–948.
[29] Han D, Williams E, Cadenas E. Mitochondrial respiratory chain-dependent generation of superoxide anion and its release into the intermembrane space. Biochem J 2001; 353: 411–416.
[30] Birch-Machin M. Assessment of mitochondrial function in vitro and *in vivo*. In: J Dykens, Y Will, editors. Drug-induced mitochondrial dysfunction. New Jersey: Wiley; 2008. p 383–396.
[31] Birch-Machin M, Howell N, Turnbull D. Defects at coupling site II. In: Jones D, Lash L, editors. Methods in toxicology. San Diego: Wiley; 1993. p 324–336.
[32] O'Malley Y, Fink BD, Ross NC, Prisinzano TE, Sivitz WI. Reactive oxygen and targeted antioxidant administration in endothelial cell mitochondria. J Biol Chem 2006; 281: 39766–39775.
[33] Lambert AJ, Brand MD. Inhibitors of the quinone-binding site allow rapid superoxide production from mitochondrial NADH:ubiquinone oxidoreductase (complex I). J Biol Chem 2004;279:39414–39420.
[34] Ohnishi ST, Ohnishi T, Muranaka S, Fujita H, Kimura H, Uemura K, Yoshida K, Utsumi K. A possible site of superoxide generation in the complex I segment of rat heart mitochondria. J Bioenerg Biomemb 2005;37:1–15.
[35] Raijmakers MT, Peters WH, Steegers EA, Poston L. NAD(P)H oxidase associated superoxide production in human placenta from normotensive and pre-eclamptic women. Placenta 2004;25(Suppl A):S85–S89.
[36] Doughan AK, Dikalov SI. Mitochondrial redox cycling of mitoquinone leads to superoxide production and cellular apoptosis. Antioxid Redox Sgnal 2007;9:1825–1836.
[37] Fridovich I. Superoxide radical and superoxide dismutases. Annu Rev Biochem 1995;64:97–112.
[38] Okado-Matsumoto A, Fridovich I. Subcellular distribution of superoxide dismutases (SOD) in rat liver: Cu,Zn-SOD in mitochondria. J Biol Chem 2001;276:38388–38393.
[39] Meany DL, Thompson L, Arriaga EA. Simultaneously monitoring the superoxide in the mitochondrial matrix and extramitochondrial space by micellar electrokinetic chromatography with laser-induced fluorescence. Anal Chem 2007;79:4588–4594.
[40] Inarrea P, Moini H, Rettori D, Han D, Martinez J, Garcia I, Fernandez-Vizarra E, Iturralde M, Cadenas E. Redox activation of mitochondrial intermembrane space Cu,Zn-superoxide dismutase. Biochem J 2005;387:203–209.
[41] Griendling KK, FitzGerald GA. Oxidative stress and cardiovascular injury: part I: Basic mechanisms and *in vivo* monitoring of ROS. Circulation 2003;108:1912–1916.
[42] Stokes KY, Clanton EC, Russell JM, Ross CR, Granger DN. NAD(P)H oxidase-derived superoxide mediates hypercholesterolemia-induced leukocyte-endothelial cell adhesion. Circ Res 2001;88:499–505.
[43] Taylor RW, Birch-Machin MA, Bartlett K, Lowerson SA, Turnbull DM. The control of mitochondrial oxidations by complex III in rat muscle and liver mitochondria. Implications for our understanding of mitochondrial cytopathies in man. J Biol Chem 1994;269:3523–3528.

This paper was first published online on iFirst on 25 June 2009.